Broadly tunable femtosecond Cr:LiSAF laser

D. Kopf, A. Prasad, G. Zhang, M. Moser,* and U. Keller

Ultrafast Laser Physics, Institute of Quantum Electronics, Swiss Federal Institute of Technology, ETH Hönggerberg-HPT, CH-8093 Zürich, Switzerland

Received November 25, 1996

We demonstrate wavelength tunability of femtosecond pulses over a range of more than 50 nm from a diode-pumped Cr:LiSAF laser. The mode-locking mechanism can be explained by soliton mode locking that is started and stabilized by a broadband semiconductor saturable-absorber mirror designed for low loss over the full reflection bandwidth of the underlying Bragg mirrors, which ultimately limits tunability. We obtain 45-fs pulses at 105-mW average output power and a maximum mode-locked average output power of 125 mW with 60-fs pulses. © 1997 Optical Society of America

Diode-pumped broadband lasers are of special interest for a number of practical applications. Cr:LiSAF (Ref. 1) has a fluorescence linewidth similar to that of Ti:sapphire and can be pumped at wavelengths near 670 nm, at which commercial high-brightness, high-power (i.e., <0.5 W) diode arrays are available. However, these crystals have a stronger tendency for upper-state lifetime quenching[2] and suffer from lower thermal conductivity, resulting in nonideal performance (limited average power) at relatively low pump powers. At present, the shortest pulses of ≈ 20 fs have been obtained with Kerr-lens mode-locked (KLM) Cr:LiSAF (Refs. 3 and 4) with an average output power of ≈ 1 mW. Higher output power has been achieved only at the expense of longer pulses. For example, 40-fs pulses with an average output power of 70 mW have recently been obtained[4] with a KLM Cr:LiSAF laser. KLM is inherently broadband because the effective saturable absorption is based on a nonresonant nonlinearity, i.e., the Kerr effect. Therefore, a tunability of 50 mm (Ref. 5) to 60 nm (Ref. 3) has been demonstrated with a femtosecond KLM Cr:LiSAF laser.

Self-starting pulse generation without critical cavity alignment can be obtained with different semiconductor saturable-absorber mirrors[6] (SESAM's). However, in this case the saturable absorption is based on a resonant nonlinearity, i.e., band filling, which tends to limit tunability. Initially, in 1994, Mellish *et al.*[7] used a SESAM inside the main cavity, producing pulses as short as 220 fs but with only a few milliwatts of output power owing to the relatively high losses of their saturable-absorber design.[7] Shortly afterward, we demonstrated[8,9] significantly higher average output power of 140 mW cw and 50 mW mode locked with pulses as short as 98 fs, using two 0.4-W high-brightness diode arrays, improved pump mode matching, and a low-loss, high-finesse antiresonant Fabry–Perot saturable absorber[6,10] (A-FPSA). Within a year, we improved the pulse duration to 45 fs with a mode-locked average output power of 60 mW and later 80 mW.[11,12] Tsuda *et al.*[13] used a saturable Bragg reflector inside a diode-pumped Cr:LiSAF laser and demonstrated 100-fs pulses with 11-mW average output power. Recently, they improved this result with a master oscillator power amplifier diode laser, which provides a near-diffraction-limited 0.5-W pump, achieving 70-fs pulses with 100-mW output power.[14] The saturated Bragg reflector is a special low-finesse A-FPSA design for which the optical thickness $\bar{n}d$ in Fig. 1 is a quarter-wavelength $\lambda/4$, and its transparent spacer layers are AlGaAs instead of AlAs, such that these last layers can be considered to be part of the lower Bragg mirror. A more detailed discussion of the different SESAM designs is given in Ref. 6.

In this Letter we present another special SESAM design, a broadband low-finesse A-FPSA (Fig. 1), with which we obtained more than 50-nm tunability with pulses as short as 45 fs and average powers as great as 125 mW from a diode-pumped Cr:LiSAF laser, using two 0.5-W high-brightness 100-μm stripe-width diode arrays. The tunability was limited by the lower AlAs/AlGaAs Bragg mirror bandwidth of the SESAM device. These results can be described by soliton mode locking.[15,16] Basically, we demonstrate here that we

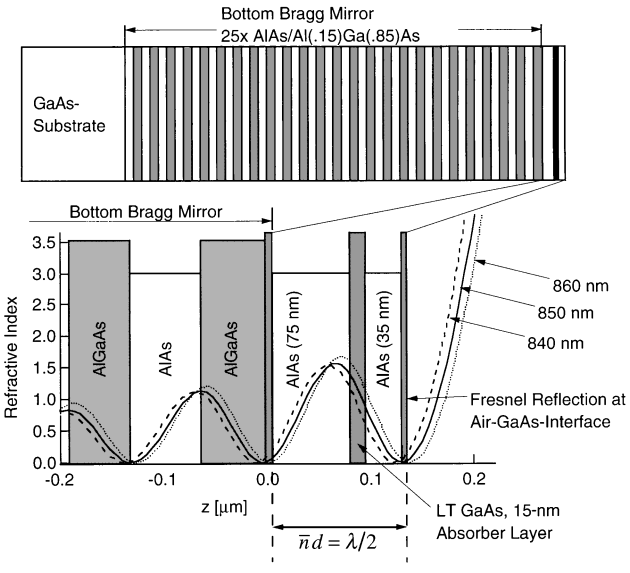

Fig. 1. Structure of the broadband low-finesse A-FPSA with an expanded view of the top layers of the structure, including the standing-wave intensity patterns for three different wavelengths with the same intensity incident upon the device. LT, low-temperature grown; z, position vertical to sample surface.

0146-9592/97/090621-03$10.00/0

can combine the benefits of SESAM's, such as self-starting mode locking and uncritical cavity alignment, with broad wavelength tunability.

The responsible nonlinearity of our intracavity SESAM devices is absorption bleaching, which has an inherent wavelength-dependent absorption. However, with soliton mode locking[15,16] we can relax the requirements on the semiconductor saturable-absorber recovery time, which only has to be sufficiently fast to stabilize the soliton. The recovery time typically can be roughly 10 times slower than the steady-state pulse duration, depending mainly on the gain and net negative dispersion in the laser.[17] Therefore, we do not have to operate at the fast but narrow-band excitonic nonlinearity.

The broadband SESAM device is based on a low-finesse A-FPSA design (Fig. 1), in which a single 15-nm-thick GaAs absorber quantum well with a bandgap wavelength of $\approx$860 nm is placed within a half-wavelength-thick transparent AlAs spacer layer in such a way that the standing-wave intensity dependence partially compensates for the wavelength dependence of the absorption edge. Low-temperature molecular beam epitaxy growth at $\approx$400 °C further broadens the absorption edge of GaAs. This results in a relatively flat wavelength dependence of the low-intensity reflectivity of the low-finesse A-FPSA, which is $\approx$98.5% with a variation in reflectivity of less than $\pm$0.7% across the whole bandwidth of the Bragg mirror. According to our calculations, the structure would show a decrease in reflectivity of $\sim$4–5% at the lower wavelength if the absorber layer were located at the standing-wave peak, i.e., $\sim$20 nm further inside (while the Fabry–Perot thickness was kept at antiresonance). This would introduce too much loss for a low-gain Cr:LiSAF laser. The thickness of the GaAs absorber layer was limited by the residual nonsaturable losses. The half-wave optical thickness of the absorber, $\bar{n}d = \lambda/2$ in Fig. 1, and the AlAs spacer layer adjusts the Fabry–Perot thickness for antiresonance (i.e., round-trip phase adjusted for destructive interference), and therefore broadband reflectivity. The Fabry–Perot cavity is formed by the lower AlAs/$Al_{0.15}Ga_{0.85}As$ Bragg mirror and the Fresnel reflection of the semiconductor–air interface. The round-trip phase shift of 3π is determined by the π-phase shift at the lower Bragg mirror, the half-wave optical thickness, and the zero-phase at the semiconductor–air interface (Fig. 1). The residual reflections at the AlAs/GaAs interfaces are negligible. The thin 5-nm GaAs layer on both the Bragg mirror and the last AlAs layer reduces oxidation effects but introduces negligible absorption because these GaAs layers are at a node of the standing wave. We typically grow the lower Bragg mirror with metal-organic chemical-vapor deposition during a separate growth run, followed by molecular beam epitaxy regrowth for the rest of the structure.

An alternative approach to achieve approximately constant absorption–reflection of the SESAM over a broad wavelength range was demonstrated with a thick saturable-absorber layer that can be integrated inside a high-finesse A-FPSA design. In this case we continually varied the bandgap of an $Al_xGa_{1-x}As$ saturable-absorber layer during semiconductor growth by varying the Al concentration.[18] Another alternative is to change the temperature of the SESAM. This shifts the bandgap and results in tunability over a few tens of nanometers. This method can be used if, for example, saturable absorption at the exciton peak, which spreads over only a few nanometers, is used as the mode-locking mechanism. However, this method again adds more complexity to the system.

The laser setup is shown in Fig. 2. We use an asymmetric cavity design with a 2-mm-long, 3% Cr-doped LiSAF crystal (Lightning Optical Corporation, Tarpon Springs, Fla.), two 10-cm radius-of-curvature laser mirrors, an SF10-prism sequence followed by a 0.8% output coupler, and the low-finesse A-FPSA as a flat end mirror of the other, shorter cavity arm. The distance between the two curved mirrors is 12.6 cm, such that the lasing mode radius on the saturable absorber is 50 μm $\times$ 55 μm, according to *ABCD* matrix calculations. The cavity repetition rate is 176 MHz. The pump-focusing optics is similar to that in Ref. 9 where we used a cylindrical micro lens, followed by two doublets that first collimate and then refocus the diode light. The two 500-mW, 100-μm stripe-width laser diodes deliver a total absorbed pump power of 700 mW at the laser crystal. The relatively high doping (3%) of the laser medium did not cause any significant decrease in performance as a result of upper-state lifetime quenching[2] or upconversion[19] because of the low intracavity loss. In the case of higher loss, and thus higher laser threshold, the laser performance would be expected to be significantly more sensitive to the crystal heat-sink temperature.[9] We kept the laser crystal heat sink at a temperature of 20 °C.

Both the mode locking and tuning results are shown in Fig. 3. The bottom graph shows different self-starting mode-locked pulse spectra as the center wavelength is tuned. We tune the laser wavelength by moving an adjustable-slit aperture in the spatially dispersed beam at the end of the resonator arm containing the prism pair. At each data point, we increase the insertion of one of the intracavity prisms to optimize

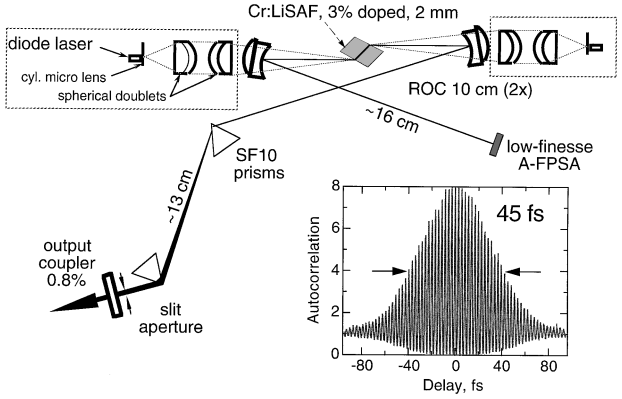

Fig. 2. Femtosecond diode-pumped Cr:LiSAF laser setup. The graph is an autocorrelation of the shortest pulses obtained at an average output power of 105 mW. The corresponding spectrum is shown as a solid curve in Fig. 3. ROC, radius of curvature.

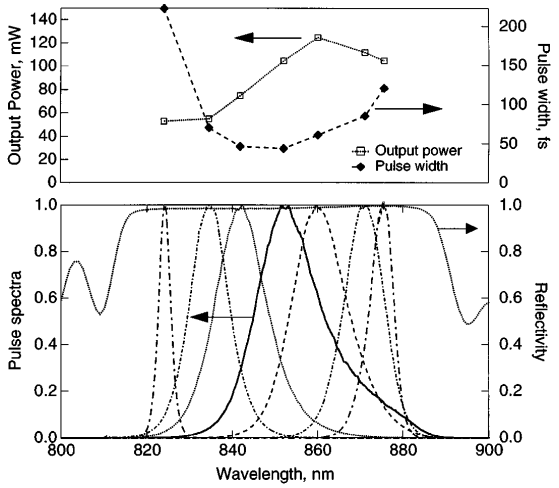

Fig. 3. Bottom: Different pulse spectra as the center wavelength is tuned by a moving-slit aperture (left-hand scale), and measured reflectivity of the broadband low-finesse A-FPSA with a variation of less than 1.5% over the tuning range (dotted curve, right-hand scale). Top: Corresponding measured pulse widths (right-hand scale) and output powers (left-hand scale).

for the shortest pulse duration. The tuning range is limited by the lower Bragg mirror of the low-finesse A-FPSA. We obtain the shortest pulse of 45 fs (graph in Fig. 2) at a center wavelength of 850 nm (corresponding to the solid curve in Fig. 3) and an average output power of 105 mW. The highest mode-locked output power is 125 mW with 60-fs pulses at a center wavelength of 860 nm. The top graph in Fig. 3 shows the corresponding measured pulse widths and average output power.

Soliton mode locking[15,16] provides a good explanation for the dominant pulse-formation process, because we do not rely on any critical cavity alignment and the recovery time of the saturable absorber is significantly longer than the pulse duration. We characterized the impulse response of the low-finesse A-FPSA with a standard noncollinear degenerate pump-probe measurement, using 100-fs pulses from a Ti:sapphire laser. We determined a fast recovery time of more than 400 fs at 830, 845, and 862 nm at an excitation level slightly below the saturation fluence of the device. This is nearly 10 times longer than the shortest pulses. The slow recovery time was several picoseconds for all wavelengths. We measured a saturation fluence of $\approx 160\ \mu J/cm^2$ at 830 nm, a maximum modulation depth of 1.4%, and a nonsaturable loss of 1%.[20] These values did not change significantly with wavelength. At 100-mW average output power the incident pulse energy density on the low-finesse A-FPSA inside the laser resonator is $\approx 800\ \mu J/cm^2$, which is ~ 5 times greater than the saturation fluence of the device. These high excitation densities are well above the exciton saturation level, and we can neglect any excitonic nonlinearities.

In conclusion, we have demonstrated a semiconductor saturable-absorber mirror (SESAM) design based on a low-finesse A-FPSA structure that is optimized for broad wavelength tunability of femtosecond pulses. The proposed structure is simple both in design and fabrication. We demonstrated tunability over more than 50 nm from a diode-pumped Cr:LiSAF laser with a maximum mode-locked output power of 125 mW (60 fs) and achieved a minimum pulse duration of 45 fs (105 mW).

We thank Thierry Strässle, ETH Zürich, for help with the experiments. This work was supported by the Swiss National Science Foundation.

*Permanent address, Paul Scherrer Institute, Zürich, Switzerland.

References

1. S. A. Payne, L. L. Chase, L. K. Smith, W. L. Kway, and H. Newkirk, J. Appl. Phys. **66,** 1051 (1989).
2. M. Stalder, M. Bass, and B. H. T. Chai, J. Opt. Soc. Am. B **9,** 2271 (1992).
3. M. J. P. Dymott and A. I. Ferguson, Opt. Lett. **20,** 1157 (1995).
4. R. Mellish, N. P. Barry, S. C. W. Hyde, R. Jones, P. M. W. French, J. R. Taylor, C. J. v. d. Poel, and A. Valster, Opt. Lett. **20,** 2312 (1995).
5. F. Falcoz, F. Balembois, P. Georges, and A. Brun, Opt. Lett. **20,** 1874 (1995).
6. U. Keller, K. J. Weingarten, F. X. Kärtner, D. Kopf, B. Braun, I. D. Jung, R. Fluck, C. Hönninger, N. Matuschek, and J. Aus der Au, IEEE J. Sel. Topics Quantum Electron. **2** (1996).
7. P. M. Mellish, P. M. W. French, J. R. Taylor, P. J. Delfyett, and L. T. Florez, Electron. Lett. **30,** 223 (1994).
8. D. Kopf, K. J. Weingarten, L. Brovelli, M. Kamp, and U. Keller, in *Conference on Lasers and Electro-Optics*, Vol. 8 of 1994 OSA Technical Digest Series (Optical Society of America, Washington, D.C., 1994), paper CPD22.
9. D. Kopf, K. J. Weingarten, L. Brovelli, M. Kamp, and U. Keller, Opt. Lett. **19,** 2143 (1994).
10. U. Keller, D. A. B. Miller, G. D. Boyd, T. H. Chiu, J. F. Ferguson, and M. T. Asom, Opt. Lett. **17,** 505 (1992).
11. D. Kopf, K. J. Weingarten, L. R. Brovelli, M. Kamp, and U. Keller, in *Conference on Lasers and Electro-Optics*, Vol. 15 of 1995 OSA Technical Digest Series (Optical Society of America, Washington, D.C., 1995), paper CWM2.
12. D. Kopf, T. Strässle, G. Zhang, F. X. Kärtner, U. Keller, M. Moser, D. Jubin, K. J. Weingarten, R. J. Beach, M. A. Emanuel, and J. A. Skidmore, Proc. SPIE **2701,** 11 (1996).
13. S. Tsuda, W. H. Knox, E. A. de Souza, W. Y. Jan, and J. E. Cunningham, Opt. Lett. **20,** 1406 (1995).
14. S. Tsuda, W. H. Knox, and S. T. Cundiff, Appl. Phys. Lett. **69,** 1538 (1996).
15. F. X. Kärtner and U. Keller, Opt. Lett. **20,** 16 (1995).
16. F. X. Kärtner, I. D. Jung, and U. Keller, IEEE J. Sel. Topics Quantum Electron. **2** (1996).
17. I. D. Jung, F. X. Kärtner, L. R. Brovelli, M. Kamp, and U. Keller, Opt. Lett. **20,** 1892 (1995).
18. G. R. Jacobovitz-Veselka, U. Keller, and M. T. Asom, Opt. Lett. **17,** 1791 (1992).
19. S. A. Payne, L. K. Smith, R. J. Beach, B. H. T. Chai, J. H. Tassano, L. D. DeLoach, W. L. Kway, R. W. Solarz, and W. F. Krupke, Appl. Opt. **33,** 5526 (1994).
20. L. R. Brovelli, U. Keller, and T. H. Chiu, J. Opt. Soc. Am. B **12,** 311 (1995).